ELSEVIER

Physica C 361 (2001) 13–21

PHYSICA C

www.elsevier.com/locate/physc

$Bi_2Sr_2Ca_{n-1}Cu_nO_{2(n+2)+\delta}$ thin films on c-axis oriented and vicinal substrates

R. Rössler [a], J.D. Pedarnig [a,*], Ch. Jooss [b]

[a] *Angewandte Physik, Johannes-Kepler-Universität Linz, A-4040 Linz, Austria*
[b] *Institut für Materialphysik, Universität Göttingen, D-37073 Göttingen, Germany*

Received 4 January 2001; received in revised form 6 March 2001; accepted 27 March 2001

Abstract

$Bi_2Sr_2Ca_{n-1}Cu_nO_{2(n+2)+\delta}$ ($n = 1, 2, 3$) thin films are prepared on c-axis oriented and vicinal substrates by pulsed-laser deposition. Optimization of substrate temperature, laser fluence and post-annealing conditions produces single-phase, well-oriented and smooth films. The surface morphology, texture, crystallinity and stoichiometry of $Bi_2Sr_2CaCu_2O_{8+\delta}$ (Bi-2212) thin films strongly depend on the fabrication parameters. On (0 0 1) $SrTiO_3$ substrates, c-axis oriented Bi-2212 films with J_c (60 K) $= 2 \times 10^6$ A/cm^2 and $T_{c0} = 82$ K are obtained. Vicinal Bi-2212 films grown on miscut substrates reveal anisotropic resistivities independent of film thickness (20–300 nm), high J_c anisotropy and strong in-plane and out-of-plane texture. © 2001 Elsevier Science B.V. All rights reserved.

PACS: 74.76.Bz; 74.72.Hs; 81.15.Fg
Keywords: Bi-based cuprates; Vicinal thin films; Pulsed-laser deposition

1. Introduction

The $Bi_2Sr_2Ca_{n-1}Cu_nO_{2(n+2)+\delta}$ high temperature superconductor (HTS) is very important for fundamental investigations and technical applications. $Bi_2Sr_2Ca_{n-1}Cu_nO_{2(n+2)+\delta}$ (BSCCO) has high critical temperatures ($T_{c0} \sim 85$ K ($n = 2$) and $T_{c0} \sim 110$ K ($n = 3$)) and high critical current densities at low temperature and is used for the fabrication of long lengths HTS tapes. The strong anisotropy of this compound and the easy intergrowth of different phases has challenged several groups to grow thin films with well-oriented and single-phase structure. Different techniques such as molecular beam epitaxy (MBE) [1,2], metal-organic chemical vapor deposition (MOCVD) [3, 4], sputtering [5–9], liquid phase epitaxy (LPE) [10] and pulsed-laser deposition (PLD) [11–13] ($n = 1, 2$), [14–18] ($n = 2$), [19–22] ($n = 2, 3$) have been employed. In particular, PLD allows to adjust preparation parameters independently and to deposit films of complex stoichiometries with relatively high deposition rates [23]. $REBa_{2-x}Sr_xCu_3O_{7-\delta}$ films (RE is rare earth) grown by PLD reveal different film orientation, surface morphology and electrical and superconducting properties depending on the parameters employed [24]. For the deposition of BSCCO thin films additional complexity arises from possible phase mixture

* Corresponding author. Tel. +43-732-24689246; fax: +43-732-24689242.
E-mail address: johannes.pedarnig@jk.uni-linz.ac.at (J.D. Pedarnig).

PII: S0921-4534(01)00409-9

and oxygen overdoping. Vicinal $Bi_2Sr_2CaCu_2O_{8+\delta}$ films have been grown on slightly miscut substrates to investigate the anisotropic transport properties [25,26] and the intrinsic Josephson effect [27] and to achieve *a–b* untwinning [28]. We have systematically varied the vicinal angle and obtained oriented growth for angles $\leqslant 15°$ [29]. The anisotropic resistivities were in very good agreement to single crystal data for film thickness in the range 20–300 nm [30].

In this paper the PLD of $Bi_2Sr_2Ca_{n-1}Cu_nO_{2(n+2)+\delta}$ ($n = 1$–3) thin films on *c*-axis oriented and vicinal substrates is reported. The laser fluence, growth temperature and post-annealing conditions are optimized to achieve single-phase, well oriented and smooth $Bi_2Sr_2CaCu_2O_{8+\delta}$ films with high T_{c0} and J_c values. Phase pure and oriented $(Bi,Pb)_2Sr_2Ca_2Cu_3O_{10+\delta}$ and $Bi_2Sr_2CuO_{6+\delta}$ films are produced on *c*-axis oriented substrates. Vicinal $Bi_2Sr_2CaCu_2O_{8+\delta}$ films are strongly textured and reveal markedly different electrical and superconducting properties as compared to vicinal $YBa_2Cu_3O_{7-\delta}$ films.

2. Experimental

$Bi_2Sr_2Ca_{n-1}Cu_nO_{2(n+2)+\delta}$ films with $n = 1$–3 were prepared by PLD using $Bi_2Sr_2CuO_{6+\delta}$, $Bi_2Sr_2CaCu_2O_{8+\delta}$, and $(Bi,Pb)_2Sr_2Ca_2Cu_3O_{10+\delta}$ ceramic targets, respectively. The target stoichiometries were Bi:Sr:Ca:Cu = 2.01:1.98:1.08:1.98 ($n = 2$) and Bi:Pb:Sr:Ca:Cu = 1.85:0.35:1.90:2.05:3.05 ($n = 3$) as measured by EDX (uncertainty ±5%). The relative target densities were 76% ($n = 1$), 69% ($n = 2$) and 92% ($n = 3$). For ablation KrF excimer-laser radiation ($\lambda = 248$ nm, $\tau \cong 25$ ns, $E_{pulse} \leqslant 1$ J, 1–2 Hz repetition rate) was focused onto the target surface. Circular spots of uniform laser fluence were achieved using an aperture (diameter 14 mm) and a lens system (focal length 200 mm). Spot size was 2.3 mm^2. For homogeneous target ablation and suppression of cone formation the targets were rotated and scanned simultaneously [31]. Laser ablation was performed in oxygen atmosphere.

BSCCO films were deposited on *c*-axis oriented and vicinal $SrTiO_3$ and (0 0 1) MgO substrates. The vicinal angle between substrate *c*-axis and surface normal was $\theta_S \leqslant 25°$. The substrates were mounted parallel to the target surface at a distance $d_{TS} = 58$ mm. Typically, 160–2500 laser pulses were employed for deposition. For electrical characterization by four-point measurements films were patterned (bridges 25 μm × 800 μm) using photolithography and wet-chemical etching (1–10% HNO_3). Etching deteriorated the film properties and oxygen annealing (~700°C, 1.2 mbar oxygen, 1 h) was employed to restore the film quality.

3. Results and discussion

3.1. c-axis oriented $Bi_2Sr_2Ca_{n-1}Cu_nO_{2(n+2)+\delta}$ films

$Bi_2Sr_2CaCu_2O_{8+\delta}$ (Bi-2212) thin films were grown on (0 0 1) $SrTiO_3$ and (0 0 1) MgO substrates for different substrate temperatures, laser fluences and post-annealing conditions. In first experiments the substrate temperature was varied in the range $T_S = 760$–810°C. Laser fluence $\Phi = 3.25$ J/cm^2, oxygen background pressure $p(O_2) = 2.5$ mbar, and number of laser pulses $N = 800$ were kept constant. After deposition in situ post-annealing was performed at $T_S = 770$°C and $p(O_2) = 1.2$ mbar for 90 min (MgO) and 120 min ($SrTiO_3$), respectively. All films of this series were *c*-axis oriented and revealed a single-phase XRD pattern. The *c*-axis length was $c = 30.81 \pm 0.03$ Å in good agreement with single crystal data [32]. Formation of the Bi-2201 phase was observed for $T_S < 750$°C and at temperatures $T_S > 810$°C the films became unstable. The decomposition of Bi-2212 films at the high temperatures is in agreement with results on phase stability investigations of bulk $Bi_2Sr_2CaCu_2O_{8+\delta}$ [33]. The transition temperature T_{c0} increased with increasing deposition temperature and reached a maximum at $T_S = 780$°C (Fig. 1). At higher temperatures the T_{c0} was different depending on the substrate. The onset critical temperature was in the range 90–95 K independent of T_S. The increase of T_{c0} for $T_S \leqslant 780$°C is attributed to enhanced surface diffusion of species and improved phase formation. On MgO substrates, the decrease of T_{c0} for $T_S > 780$°C may be due to internal strain [6] originating from large lattice mismatch and

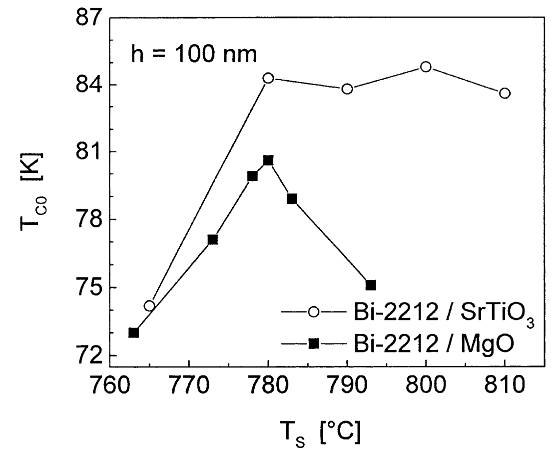

Fig. 1. Critical temperature T_{c0} of *c*-axis oriented Bi-2212 films deposited at different temperatures T_S on (0 0 1) $SrTiO_3$ and (0 0 1) MgO substrates. Laser fluence and oxygen pressure were 3.25 J/cm^2 and 2.5 mbar, respectively. Film thickness was 100 nm.

different thermal expansion coefficients. The mismatch was 9.9% and ~40% for the lattice parameters and the thermal expansion coefficients [34], respectively. For $SrTiO_3$ substrates, the mismatch was 2.3% and ~6% [34], respectively.

In a second series of experiments, Bi-2212 films were grown at fluence $\Phi = 1.5$–4.5 J/cm^2 and substrate temperatures $T_S = 780°C$ (MgO) and $T_S = 790°C$ ($SrTiO_3$). Parameters kept constant were $p(O_2) = 2.5$ mbar, $N = 800$ and post-annealing conditions $p(O_2) = 1.2$ mbar, $T_S = 770°C$, 120 min. Formation of cracks on the target surface was observed for $\Phi > 4.5$ J/cm^2 and ablation was stopped to avoid target fragmentation. At the lowest fluence employed films were strongly non-stoichiometric showing Bi and Ca enrichment and Cu and Sr depletion. At higher fluences (2.5–4 J/cm^2) both the enrichment and the depletion of different elements decreased and stoichiometry was Bi:Sr:Ca:Cu = 2.1:1.9:1.2:1.8 (uncertainty ±10%) for 3.25 J/cm^2. Enrichment of Bi in laser deposited Bi-2212 films was reported previously [35]. Fig. 2 shows the dependence of T_{c0}, J_c and particulate formation on laser fluence. A strong increase of T_{c0} with increasing fluence was observed and $T_{c0} > 82$ K was obtained for $\Phi \geqslant 3$ J/cm^2. The critical current density showed a moderate fluence dependence for films grown on $SrTiO_3$ substrates. For

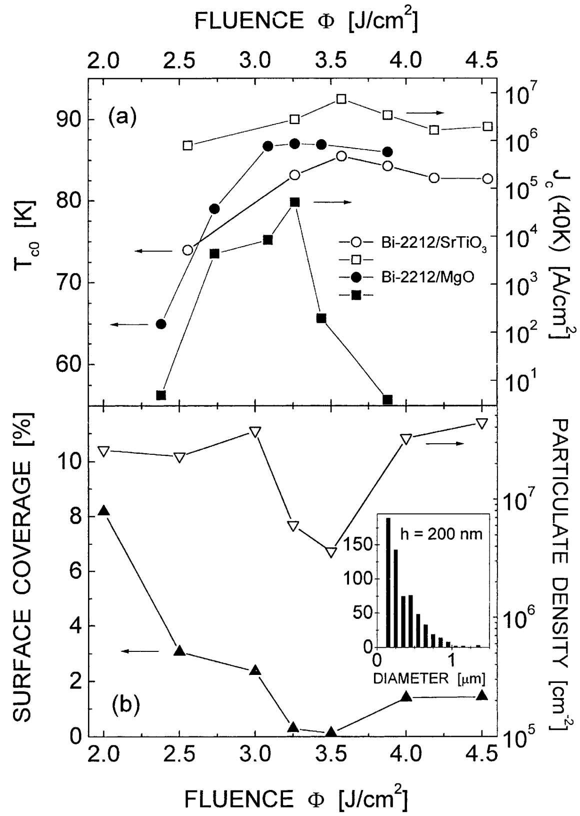

Fig. 2. (a) Critical temperature T_{c0} and critical current density J_c (40 K) of *c*-axis oriented Bi-2212 films deposited at different laser fluences. (b) Film surface coverage and particulate density for different fluence. The inset shows the particulate diameter histogram for a Bi-2212/$SrTiO_3$ film of 200 nm thickness.

$\Phi = 3.25$ J/cm^2, the current density was 1×10^7, 6×10^6 and 2×10^6 A/cm^2 at $T = 20$, 40 and 60 K, respectively. On MgO substrates, the J_c was much lower and revealed a strong dependence on fluence. Particulates on the films consisted of droplets, irregularly shaped particles and outgrowths. The density of particulates with diameter $\geqslant 100$ nm was 3×10^6 cm^{-2} for $\Phi = 3.5$ J/cm^2 and increased for lower and higher fluence. The surface coverage showed a minimum of 0.2% at the same fluence level. The large coverage at low fluences was mainly due to the formation of large outgrowths. At 3.5 J/cm^2 fluence only few particulates had diameters >1 μm (inset Fig. 2). The formation of particulates has been extensively studied for different target and substrate materials and PLD systems [36].

Particulates are formed mainly by the ejection of particles from the target and the growth of precipitates on the film. Vapor phase condensation produces clusters which are typically smaller than 20 nm in diameter [24]. A strong fluence dependence of T_{c0} and J_c was observed also for $YBa_2Cu_3O_{7-\delta}$ (YBCO) layers [37]. Different mechanisms related to the ablation process, gas phase interactions and desorption from the film surface may contribute to the observed behavior. The energy, chemical state and stoichiometry of film-forming species and the deposition rate vary with fluence. The observed dependence of J_c on the substrate material is attributed to a different film texture and morphology. Good in-plane alignment of films was observed on $SrTiO_3$ substrates but multiple in-plane orientations developed on MgO [6]. Relatively smooth films with a surface roughness $\Delta h_{rms} \cong 10$ nm, grain size around 300 nm and a low particulate density were obtained on $SrTiO_3$ (Fig. 3a and c). On MgO substrates, Bi-2212 films had $\Delta h_{rms} \cong 15$ nm and many micro-cracks with widths $\leqslant 100$ nm and depths comparable to the film thickness (Fig. 3b).

For Bi-2212 films grown at $\Phi = 3.25$ J/cm^2, $T_S = 790$°C and $p(O_2) = 2.5$ mbar the deposition

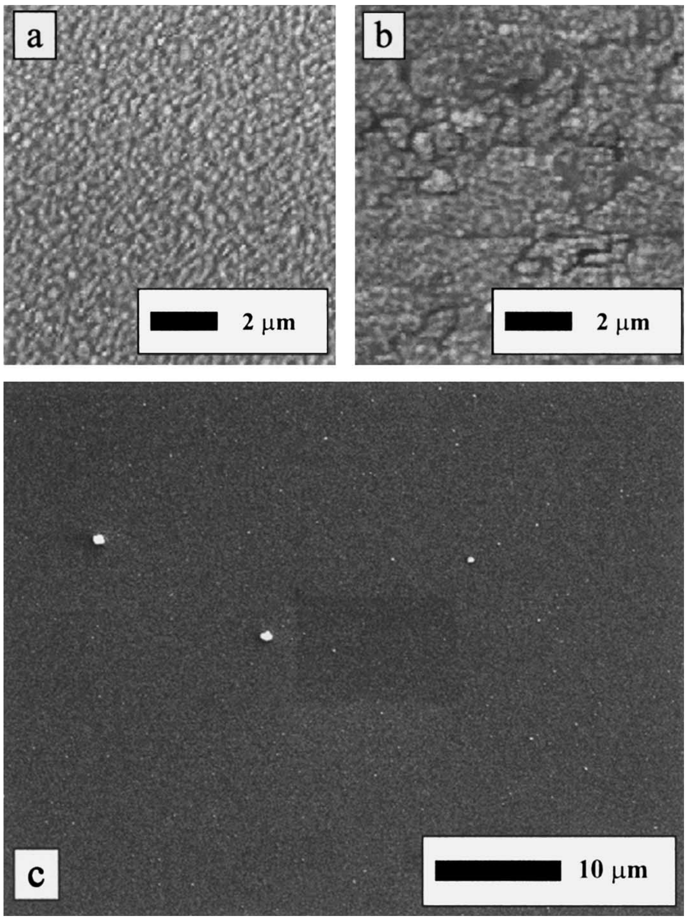

Fig. 3. Topography of Bi-2212 films deposited on (0 0 1) $SrTiO_3$ (a, c) and (0 0 1) MgO substrates (b). AFM images (a, b) show crack formation for films grown on MgO. The surface roughness is ~10 nm and ~15 nm for $SrTiO_3$ and MgO substrates, respectively. The SEM image (c) reveals a low particulate density of $\sim 3 \times 10^6$ cm^{-2} . This image was taken at an angle of 45°.

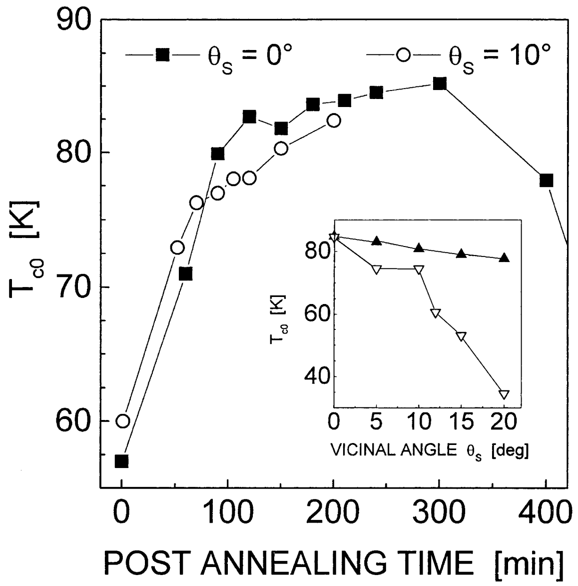

Fig. 4. In situ post-annealing of c-axis oriented ($\theta_S = 0°$) and vicinal ($\theta_S = 10°$) Bi-2212 films at 770°C in 1.2 mbar oxygen. At higher angles θ_S the T_{c0} of films deposited under optimized conditions only slightly decreases (closed symbols, inset).

rate was ~1.2 Å/pulse. Such films had $T_{c0} < 60$ K when cooled to room temperature with a rate of 20°C/min after deposition. In situ post-annealing of c-axis oriented ($\theta_S = 0°$) and vicinal ($\theta_S = 10°$) Bi-2212 films for 120 min increased the critical temperature up to $\geqslant 80$ K (Fig. 4). Prolonged annealing (120–300 min) only moderately increased T_{c0}. Very long heat treatment ($\geqslant 400$ min) decreased T_{c0} and films were non-superconducting after 12 h. XRD measurements revealed improved signal/background ratio and reduced widths of (0 0 l) reflections of annealed films. Qualitatively the same results were achieved for films on MgO and $SrTiO_3$ substrates.

The phase-pure growth of Bi-2212 films on MgO substrates within a narrow temperature range is in qualitative agreement to earlier results [12]. Zhu et al. reported $T_{c0} = 71$ K and J_c (50 K) $\sim 8 \times 10^5$ A/cm^2 for films deposited at $\Phi \sim 2$ J/cm^2, $T_S \sim 740$°C and $p(O_2) = 0.2$ mbar, and rapidly cooled after deposition without post-annealing. Our results demonstrate that in situ post-annealing and the optimization of laser fluence and substrate temperature are required to increase the critical temperature $T_{c0} > 80$ K, to strongly reduce the particulate formation and to improve the film crystallinity. c-axis oriented Bi-2212 films on $SrTiO_3$ substrates reveal improved texture, surface morphology, and J_c values as compared to films grown on MgO. The T_{c0} and J_c values of Bi-2212/$SrTiO_3$ films are comparable to results reported by Arnold et al. [16].

$(Bi,Pb)_2Sr_2Ca_2Cu_3O_{10+\delta}$ (Bi-2223) targets were used for the deposition of Bi-2223 films on (0 0 1) MgO substrates. The deposition temperature was varied in the range $T_S = 740$–810°C. Laser fluence $\Phi = 3.25$ J/cm^2 and oxygen background $p(O_2) =$ 2.5 mbar were employed. Fig. 5 shows details of

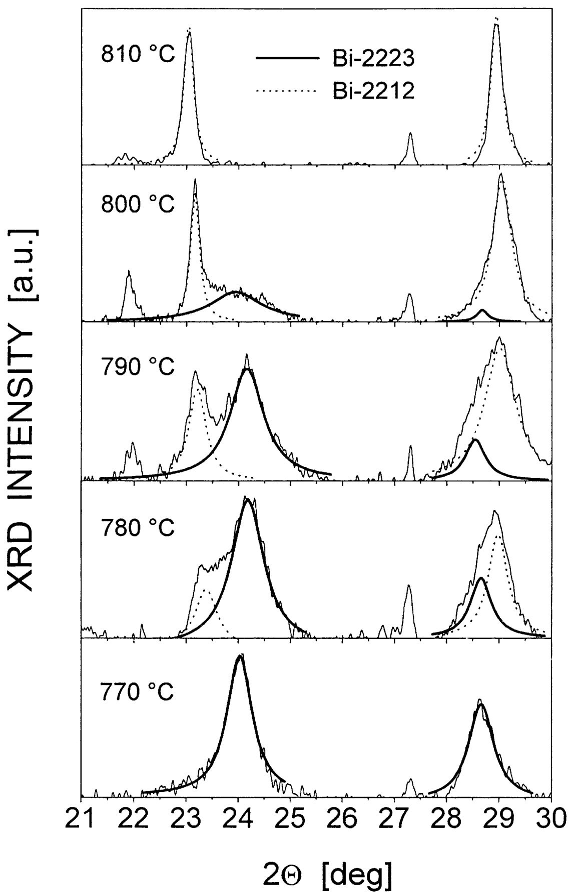

Fig. 5. XRD patterns of BSCCO films deposited at different substrate temperatures using a (Bi,Pb)-2223 target for ablation ($\Phi = 3.25$ J/cm^2). The solid and dotted lines represent Lorentz profile fits of the Bi-2223 and Bi-2212 reflections, respectively.

the XRD patterns (CuK_α) of c-axis oriented films. In the range $21° \leqslant 2\theta \leqslant 30°$ up to five $(0\,0\,l)$ reflections of different BSCCO phases are observed. For temperatures $T_S = 740$–770°C Bi-2223 is the dominant phase and (0 0 10) and (0 0 12) reflections are detected at $2\theta = 24.03°$ and 28.67°, respectively. The peak at 27.3° is due to the sample holder. At higher temperatures phase competition occurs and Bi-2212 formation is increasingly enhanced. A minor amount of Bi-2201 phase is observed for temperatures $T_S = 790$–800°C ((0 0 6) peak at $2\theta \approx 22°$). The Bi-2234 phase was not formed. The solid and dotted lines are Lorentz profile fits for the Bi-2223 and Bi-2212 phases, respectively. The measured Bi-2223 peak positions differ slightly from literature data ($2\theta_{(0\,0\,10)} = 23.92°$ and $2\theta_{(0\,0\,12)} = 28.80°$ [38]) depending on deposition temperature. This is probably due to phase intergrowth introducing stacking faults and structural modification along the film c-axis [5,10], non-optimized oxygen stoichiometry and Pb doping.

In further experiments the laser fluence and the oxygen pressure were varied ($p(O_2) = 0.3$–3.3 mbar, $\Phi = 1.5$–4.5 J/cm^2) to produce stoichiometric Bi-2223 films with metal-like resistivities in the normal state. Substrate temperature was $T_S = 730$–760°C. For $\Phi = 2.9$ J/cm^2 and $p(O_2) = 1.6$ mbar the stoichiometry was very close to target composition and films revealed metallic resistivity behavior with $T_{c0} = 26$ K. Films cooled in 100 mbar oxygen after deposition ($p(O_2) = 2.5$ mbar, $T_S = 740$°C) had $T_{c0} = 63$ K. Ex situ annealing in air at 820°C for 10 min further raised the transition temperature ($T_c^{onset} = 118$ K, $T_{c0} = 78$ K) and strongly reduced the residual resistance $R_{res}/R_{300\ K} \approx 0$. Fast heating and cooling ramps were employed to avoid Pb and Bi evaporation and film decomposition [39]. After annealing the c-axis lattice parameter was 37.11 ± 0.07 Å. This value was slightly less than for optimally oxygen doped Bi-2223 ($c = 37.17$ Å [38]). The Bi-2223 films had particulate density of $\sim 10^8$/cm^2, surface coverage of 6.5% and an average particulate diameter of 250 ± 30 nm.

$Bi_2Sr_2Cu_1O_{6+\delta}$ (Bi-2201) films were deposited from Bi-2201 targets employing $\Phi = 2.9$ J/cm^2, $p(O_2) = 2.5$ mbar and $T_S = 740$°C. Higher deposition temperatures favored Bi-2212 phase formation. Bi-2201 films grown on (0 0 1) MgO substrates revealed c-axis orientation. The lattice parameter $c = 24.60 \pm 0.10$ Å was slightly reduced as compared to single crystals ($c = 24.70$ Å [40]). This indicates overdoping since no annealing was employed after deposition. For temperatures above 50 K the films revealed metallic resistivity behavior with a residual resistance $R_{res}/R_{300\ K} \approx 0.65$. The critical temperature was $T_c^{onset} \approx 17$ K and $T_{c0} < 10$ K.

3.2. Vicinal $Bi_2Sr_2CaCu_2O_{8+\delta}$ films

Vicinal Bi-2212 films were grown on miscut $SrTiO_3$ substrates employing the same parameters as for c-axis oriented film growth. Post-annealing increased the critical temperature to 78 and 82 K after 70 and 200 min treatment, respectively (Fig. 4). The annealing times required for high T_{c0} were much longer than estimates considering anisotropic oxygen diffusion in Bi-2212 (diffusivities $D_{ab}/D_c \sim 40$ at 770°C [41]). For films of thickness h the diffusion path length was $l_{ab}h \sim \sin\theta_S$ and annealing times less than 1 min were expected ($\tau l_{ab}^2 \sim D_{ab}$). The long-term annealing probably improved film crystallinity as was observed for non-tilted Bi-2212 films. Oxygen diffusion of post-annealed vicinal films revealed thermally activated behavior at lower temperatures (230–380°C) [42]. The critical temperature of vicinal films slightly decreased for higher tilt angles, $T_{c0}(\theta_S = 0°) = 85$ K, $T_{c0}(\theta_S = 10°) = 81$ K and $T_{c0}(\theta_S = 20°) = 78$ K (inset Fig. 4). Films deposited under non-optimized conditions ($T_S = 775$°C, $\Phi = 2.35$ J/cm^2, spot size 1 mm^2, $d_{TS} = 35$ mm) showed a much stronger suppression of the critical temperature, $T_{c0}(\theta_S = 0°) = 82$ K, $T_{c0}(\theta_S = 10°) = 50$ K and $T_{c0}(\theta_S = 20°) = 35$ K. The particulate density and surface coverage on vicinal films were $\sim 5 \times 10^5$ cm^{-2} and 0.06%, respectively.

The crystallinity of vicinal films ($\theta_S = 10°$) was investigated by XRD rocking curves (ω- and φ-scans). Fig. 6 shows ω-scans of the (0 0 10) Bi-2212 reflection for different film thickness and in-plane sample orientation. The scan angle $\omega = \theta - \theta_{Bragg}$ was measured relative to the Bragg angle

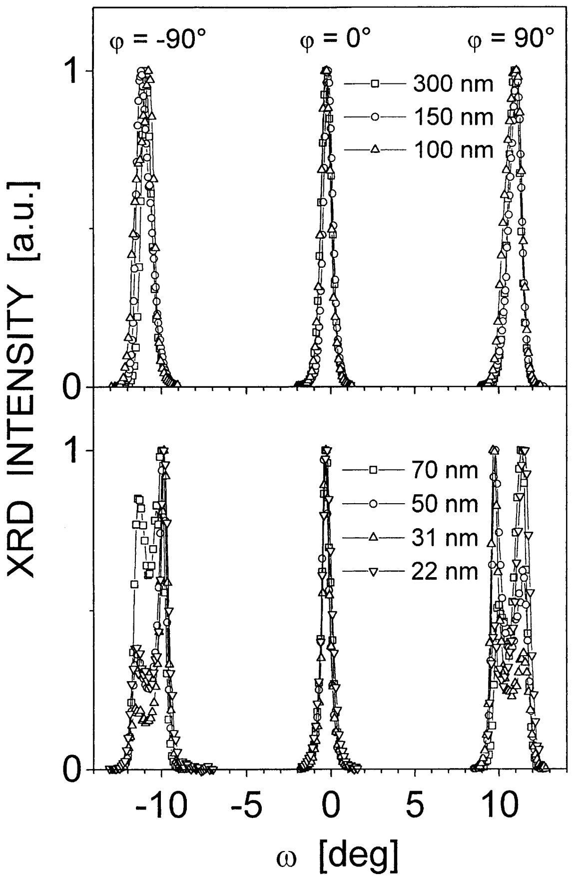

Fig. 6. XRD rocking curves of the (0 0 10) reflection of vicinal Bi-2212 films for different sample orientations (φ) and film thickness. For $\varphi = \pm 90°$ the peak intensities are observed at $\omega \approx \pm\theta_S$ due to the substrate tilt.

$\theta_{Bragg} = 23.26°$. For sample orientation $\varphi = 0°$, the film steps were aligned parallel to the plane of incidence and peaks of scattered intensity $I(\omega)$ were detected at $\omega = 0°$. The rocking curve half widths were $\Delta\omega_{FWHM} = 0.61 \pm 0.10°$ independent of film thickness in the range 20–300 nm. The width agreed well with measurements on c-oriented films ($\Delta\omega_{FWHM} = 0.65°$). For $\varphi = \pm 90°$, peak intensities were measured close to the nominal substrate tilt at $\omega = \pm(10.90 \pm 0.33)°$. Half widths were $\Delta\omega_{FWHM} = 0.78°$, $0.92°$ and $1.22°$ for film thickness $h = 300$, 150 and 100 nm, respectively. For thinner films ($\leqslant 70$ nm) the rocking curves revealed an additional peak of lower intensity. Peak positions were at $\omega = \pm(11.44 \pm 0.08)°$ and $\omega = \pm(9.86 \pm 0.11)°$. The second peak may be due to a slight change of c-axis orientation across antiphase boundaries as was observed for 15° vicinal films [43]. For all sample orientations the integrated scattering intensity, $\int I(\omega)\,d\omega$, increased linearly with film thickness. The in-plane orientation of the Bi-2212 lattice was determined from φ-scans of the (2 0 10) Bi-2212 and (1 0 1) $SrTiO_3$ peaks, respectively. A 45° rotation relative to the substrate and very strong in-plane texture were measured ($\Delta\varphi_{FWHM} = 0.66°$, Fig. 7). These results demonstrate the tilted structure of step-flow grown films and confirm results based on resistivity measurements and TEM investigations [30].

Resistivities and critical currents of vicinal Bi-2212 films were measured for current tracks oriented parallel and perpendicular to the vicinal steps ($\theta_S = 10°$). From four-point measurements the in-plane and out-of-plane resistivities ρ_{ab} and ρ_c were derived which agreed well to single crystal data [30]. The variation of ρ_c due to moderately

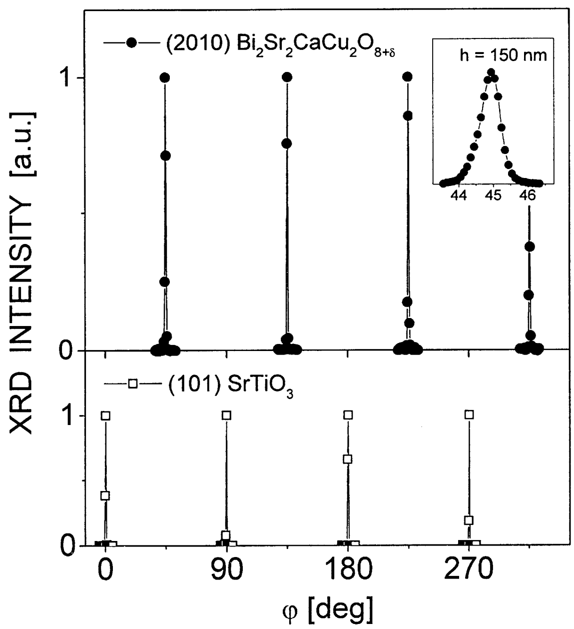

Fig. 7. XRD φ-scans of the (2 0 10) Bi-2212 and (1 0 1) $SrTiO_3$ reflections. The vicinal Bi-2212 films show a 45° in-plane rotation relative to the substrate lattice.

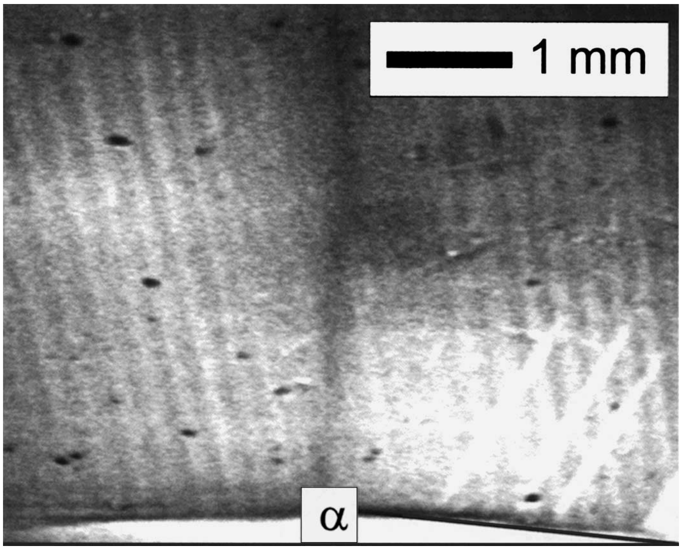

Fig. 8. Magneto-optical image of a 10° vicinal Bi-2212 film ($T = 4.2$ K, $B_{ex} = 16$ mT). The critical current anisotropy is derived from the angle α between discontinuity line and sample edge (indicated by solid lines).

different c-axis orientations was within the scatter for different films of the same thickness. The critical current densities showed strong anisotropy for measurements parallel ($J_{c,P}$) and orthogonal ($J_{c,O}$) to the vicinal steps. In zero field, $J_{c,P}(20\ \mathrm{K}) = 4 \times 10^6\ \mathrm{A/cm^2}$ and $J_{c,O}(20\ \mathrm{K}) = 3 \times 10^5\ \mathrm{A/cm^2}$ were measured for films of 120 nm thickness. The current density $J_{c,P}$ is comparable to $J_c(20\ \mathrm{K}) = 1 \times 10^7\ \mathrm{A/cm^2}$ measured on c-axis oriented films. The resistivity anisotropy and critical current anisotropy of vicinal Bi-2212 films were much higher than for vicinal YBCO films of the same tilt angle ($\theta_S = 10°$). Magneto-optical imaging of vicinal Bi-2212 films confirmed the strong critical current anisotropy (Fig. 8). Films were zero-field cooled and imaged at $T = 4.2$ K with $B_{ex} = 16$ mT. From the angle α between the discontinuity line and the sample edge the critical current anisotropy was determined $J_{c,P}/J_{c,O} = 1/\tan(\alpha) \approx 12$ in good agreement with transport data. The electrical and superconducting properties of vicinal Bi-2212 films were in remarkable contrast to vicinal YBCO films. The resistivities of YBCO films depend on film thickness in the range 60–320 nm [44]. Furthermore, critical current densities of Bi-2212 films in external magnetic fields did not reveal the force-free peak and the vortex string channeling observed in YBCO [45].

4. Conclusion

$Bi_2Sr_2Ca_{n-1}Cu_nO_{2(n+2)+\delta}$ films ($n = 1$–3) were prepared by PLD employing 248 nm KrF-excimer laser radiation for the ablation of Bi-2201, Bi-2212 and (Bi,Pb)-2223 ceramic targets. Optimization of substrate temperature, laser fluence and post-annealing produced single phase, oriented and smooth films. c-axis oriented Bi-2212 films deposited on (001) MgO and (001) $SrTiO_3$ substrates had $T_{c0} = 86$ K and $J_c\ (60\ \mathrm{K}) = 2 \times 10^6\ \mathrm{A/cm^2}$, respectively. c-axis oriented Bi-2223 and Bi-2201 films showed metallic resistivity behavior and $T_{c0} = 78$ K and $T_{c0} < 10$ K, respectively, without in situ post-annealing. Bi-2212 films grown on vicinal substrates revealed tilted structure for film thickness 20–300 nm and strong in-plane alignment. The vicinal films had anisotropic critical current densities with the higher J_c along the vicinal steps and comparable in magnitude to critical currents of epitaxial films.

Acknowledgements

We wish to thank D. Bäuerle for valuable discussions and G. Gritzner for the Bi-2223 target. Financial support under the TMR project Supercurrent (ERBFMRXCT98-0189) and the Austrian Bundesministerium für Verkehr, Innovation und Technologie is gratefully acknowledged.

References

[1] D.J. Rogers, P. Bove, F. Hosseini Teherani, Supercond. Sci. Technol. 12 (1999) R75.
[2] H. Ota, S. Migita, Y. Kasai, H. Matsuhata, S. Sakai, Physica C 311 (1999) 42.
[3] S.J. Golden, F.F. Lange, D.R. Clarke, L.D. Chang, C.T. Necker, Appl. Phys. Lett. 61 (1992) 351.
[4] T. Sugimoto, N. Kubota, Y. Shiohara, S. Tanaka, Appl. Phys. Lett. 63 (1993) 2697.
[5] Z. Mori, E. Minamizono, S. Koba, T. Doi, S. Higo, Y. Hakuraku, Physica C 339 (2000) 161.
[6] S.-I. Karimoto, S. Kubo, K. Tsuru, M. Suzuki, Jpn. J. Appl. Phys. 36 (1997) 84.
[7] M. Ohkubo, E. Brecht, G. Linker, J. Geerk, O. Meyer, Appl. Phys. Lett. 69 (1996) 574.
[8] Y. Hakuraku, S. Koba, S. Higo, A. Nakao, T. Ogushi, Supercond. Sci. Technol. 9 (1996) 23.
[9] P. Wagner, F. Hillmer, U. Frey, H. Adrian, T. Steinborn, L. Ranno, A. Elschner, I. Heyvaert, Y. Bruynseraede, Physica C 215 (1993) 123.
[10] G. Balestrino, M. Marinelli, E. Milani, A. Paoletti, P. Paroli, J. Appl. Phys. 70 (1991) 6939.
[11] L. Ranno, D. Martinez-Garcia, J. Perriere, P. Barboux, Phys. Rev. B 48 (1993) 13945.
[12] S. Zhu, D.H. Lowndes, B.C. Chakoumakos, J.D. Budai, D.K. Christen, X.-Y. Zheng, E. Jones, B. Warmack, Appl. Phys. Lett. 63 (1993) 409.
[13] T. Matsumoto, T. Kawai, K. Kitahama, S. Kawai, I. Shigaki, Y. Kawate, Appl. Phys. Lett. 58 (1991) 2039.
[14] A. Ishii, T. Hatano, Physica C 340 (2000) 173.
[15] C. Maréchal, E. Lacaze, W. Seiler, J. Perriére, Physica C 294 (1998) 23.
[16] J. Arnold, A. Pfuch, J. Borck, K. Zach, P. Seidel, Physica C 213 (1993) 71.
[17] X.F. Zhang, B. Kabius, K. Urban, P. Schmitt, L. Schultz, G. Saemann-Ischenko, Physica C 194 (1992) 253.
[18] F.S. Razavi, H.-U. Habermeier, P. Majewski, Mater. Sci. Eng. B 13 (1992) 49.
[19] N. Asano, K. Shinohara, N. Matsunami, Y. Takai, Supercond. Sci. Technol. 12 (1999) 203.
[20] A. Sajjadi, I.W. Boyd, Appl. Phys. Lett. 63 (1993) 3373.
[21] P.J. Kung, R.E. Muenchausen, J. Vac. Sci. Technol. A 11 (1993) 1354.
[22] T. Brousse, G. Poullain, J.F. Hamet, H. Murray, B. Raveau, Physica C 170 (1990) 545.
[23] D. Bäuerle, Laser Processing and Chemistry, third ed., Springer, Berlin, 2000.
[24] D. Bäuerle, Supercond. Sci. Technol. 11 (1998) 968.
[25] J.S. Tsai, J. Fujita, M.Yu. Kupriyanov, Phys. Rev. B 51 (1995) 16267.
[26] G. Balestrino, M. Marinelli, E. Milani, A.A. Varlamov, L. Yu, Phys. Rev. B 47 (1993) 6037.
[27] K. Lee, I. Iguchi, T. Ishibashi, K. Sato, Physica C 293 (1997) 212.
[28] J.N. Eckstein, I. Bozovic, D.G. Schlom, J.S. Harris Jr., Appl. Phys. Lett. 57 (1990) 1049.
[29] Th. Zahner, R. Stierstorfer, R. Rössler, J.D. Pedarnig, D. Bäuerle, H. Lengfellner, Physica C 298 (1998) 91.
[30] R. Rössler, J.D. Pedarnig, D. Bäuerle, E.J. Connolly, H.W. Zandbergen, Appl. Phys. A 71 (2000) 245.
[31] N. Arnold, D. Bäuerle, Appl. Phys. A 68 (1999) 363.
[32] A.Q. Pham, A. Maignan, M. Hervieu, C. Michel, J. Provost, B. Raveau, Physica C 191 (1992) 77.
[33] L.M. Rubin, T.P. Orlando, J.B. Vander Sande, G. Gorman, R. Savoy, R. Swope, R. Beyers, Physica C 217 (1993) 227.
[34] R. Wördenweber, Supercond. Sci. Technol. 12 (1999) R86.
[35] J. Gonzalo, C.N. Afonso, J. Perriére, Appl. Phys. Lett. 67 (1995) 1325.
[36] L.-C. Chen, in: D.B. Chrisey, G.K. Hubler (Eds.), Pulsed-Laser Deposition of Thin Films, Wiley, New York, 1994, p. 167.
[37] S. Proyer, E. Stangl, M. Borz, B. Hellebrand, D. Bäuerle, Physica C 257 (1996) 1.
[38] P.V.P.S.S. Sastry, A.R. West, Physica C 235 (1994) 503.
[39] Z.X. Zhao, G.C. Che, Appl. Supercond. 2 (3/4) (1994) 227.
[40] N.R. Khasanova, E.V. Antipov, Physica C 246 (1995) 241.
[41] M. Runde, J.L. Routbort, S.J. Rothman, K.C. Goretta, J.N. Mundy, X. Xu, J.E. Baker, Phys. Rev. B 45 (1992) 7375.
[42] A. Gramm, Th. Zahner, U. Spreitzer, R. Rössler, J.D. Pedarnig, D. Bäuerle, H. Lengfellner, Europhys. Lett. 49 (4) (2000) 501.
[43] E. Connolly, V.L. Svetchnikov, H.W. Zandbergen, J.D. Pedarnig, R. Rössler, D. Bäuerle, in: M. Ruhle, H. Gleiter (Eds.), Proceedings of EUROMAT'99, Interface Controlled Materials, vol. 9, Wiley, New York, 2000.
[44] T. Haage, J. Zegenhagen, J.Q. Li, H.-U. Habermeier, M. Cardona, Ch. Jooss, R. Warthmann, A. Forkl, H. Kronmüller, Phys. Rev. B 56 (1997) 8404.
[45] J.H. Durrell, G. Gibson, Z.H. Barber, J.E. Evetts, R. Rössler, J.D. Pedarnig, D. Bäuerle, Appl. Phys. Lett. 77 (2000) 1686.